THE JOURNAL OF PHYSICAL CHEMISTRY A

ARTICLE

pubs.acs.org/JPCA

Nuclear Magnetic Resonance Parameters for Methane Molecule Trapped in Clathrate Hydrates

Paweł Siuda and Joanna Sadlej*

Faculty of Chemistry, University of Warsaw, Pasteura 1, 02-093 Warsaw, Poland

Supporting Information

ABSTRACT: The calculations of the nuclear shielding and spin−spin coupling constants were carried out for two models of clathrate hydrates, 5^{12} and $5^{12}6^8$, using the density functional theory three-parameter Becke−Lee−Yang−Parr method with the basis set aug-cc-pVDZ (optimization) and HuzIII-su3 (NMR parameters). Particular attention has been devoted to evaluate the influence of a geometrical arrangement, the effect of long-range interactions on the NMR shielding of methane molecule, and to predict whether ^{13}C and ^{1}H chemical shifts can distinguish between guests in two clathrate hydrates cages. The correlation of the changes in the ^{17}O shielding constants depend strongly on the hydrogen-bonding topology. The intermolecular hydrogen-bond transmitted $^{1h}J_{OH}$ spin−spin coupling constants are substantial. The increase of their values is connected with the elongation of the intramolecular O−H bond and the shortening of the intermolecular O···H distance. These data suggests that hydrogen bonds between double donor−single acceptor (DDA)-type water molecules acting as a proton acceptor from single donor−double acceptor (DAA)-type water molecules are stronger than ones formed by DAA-type water molecules acting as an acceptor for a DDA water proton. These state-of-the-art calculations confirmed the earlier experimental findings of the cage-dependency of ^{13}C chemical shift of methane.

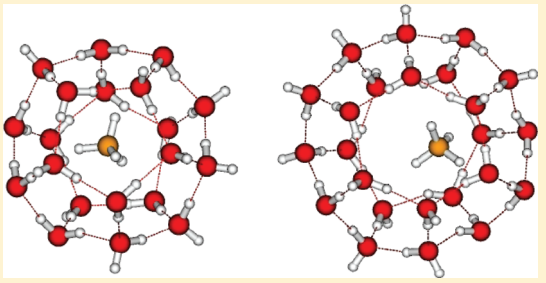

I. INTRODUCTION

Clathrate hydrates (CH) are a class of three-dimensional inclusion compounds with cages formed by water molecules. In these icelike crystalline solids the cage topology is identical to buckminsterfullerene. The CH cavities are considered unstable when empty but become stable when filled with small molecules. There are three main CH structures, namely, sI, sII, and sH, formed by five types of water cages.[1,2] The type sI unit cell is made up of 8 polyhedral cages: two pentagonal dodecahedral (20 water molecules), denoted 5^{12} with average cavity radius 3.95 Å and six tetrakaidecahedral cages denoted $5^{12}6^2$ (24 water molecules) with average cavity radius 4.33 Å. Unit cells of type sII hydrates are made up of 24 polyhedral cages: 8 hexakaidecahedrons $5^{12}6^4$ and 16 pentagonal dodecahedrons 5^{12}. The sH type unit cell contains six polyhedral cages: one large $5^{12}6^8$ (ca. 5.71 Å), three medium $4^35^{12}6^3$ (ca. 4.06 Å), and two small 5^{12} (ca. 3.91 Å).[3] The base of the notation designates the type of face, while the exponent the number of faces of the same type.

It has been demonstrated both experimentally (employing macroscopic and microscopic techniques) and theoretically (ab initio, molecular dynamics and Monte Carlo simulations) that there is a great number of host molecules effectively stabilizing CH structures. Important characteristics of those molecules include low polarity and proper size. There is a great variety of known CHs of noble gases (Ne, Ar, Kr, Xe), small homo- and heteronuclear molecules (N_2,CO,CO_2), as well as hydrocarbons and other organic molecules (CH_4, formaldehyde, tetrahydrofuran).[4−13]

Natural gas hydrates are considered to be an unexploited fuel source for the future, while synthetic hydrates are recognized as novel materials (hydrogen storage, cool energy storage, carbon dioxide sequestration).[4]

Natural methane CHs generally form structure sI under low pressure. However, by use of proper conditions it is also possible to obtain a methane CH structure sII. At high pressure (ca. 0.6 GPa) methane clathrate shows a phase transition to the sH form.[14] Methane storage in structure sH is attractive due to the relatively higher stability of sH as compared to sI structure.[4]

In the sI methane clathrate almost all small and large cages are occupied by a single methane guest molecule. Spectroscopic experiments can distinguish between methane molecules in small and large cages.[15] Two Raman bands with the intensity ratio of ca. 1:3 is registered from methane molecules from two types of cages.[16] Measurements of ^{13}C nuclear magneitc resonance (NMR) spectra shifts of guest molecules in sII CHs show two signals from two cages and ab initio HF/6-31G(d,p) calculations reproduce these data.[17] Two signals with an intensity ratio 1:3.72 can be seen for methane on the ^{13}C NMR spectra,[17,18] too. Stability and preferred structures of CH with methane as a guest molecules has been studied by ab initio (Hartree−Fock, Møller−Plesset perturbation theory (MP2)) and density functional theory (DFT) calculations.[5,19,20]

Received: November 5, 2010
Revised: December 17, 2010

Proton-shielding constants for hydrogen guests in small and large cages of structure II have been studied by Alavi et al.[21]

The parameters of NMR spectra are sensitive probes of the electronic structure of molecules, intermolecular interactions, and the influence of the environment.[22,23] The most widely used parameters in such studies are the isotropic and anisotropic shielding constants. The indirect (scalar) spin−spin coupling constants (SSCCs) are of particular importance in structural studies due to their sensitivity to conformational changes. On the other hand, developments in experimental NMR technique also enable measurements of both parameters.

In our previous papers we have paid special attention to the shielding constants and SSCCs for ^{17}O and ^{1}H nuclei in water molecules in different clusters $(H_2O)_n$, $n = 2-6$, 12, 17 calculated at the B3LYP/aug-cc-pCVDZ level.[24,25] Many important properties of hydrogen-bonded networks depend on the hydrogen-bonding topology of the network. Not only the energy but also the spectroscopic and dynamical coupling between hydrogen bonds can vary significantly due to cooperative effects. The main structural units in water clusters $n \geq 6$ are three-coordinated water molecules of the two varieties: the double donor−single acceptor (DDA) and the single donor−double acceptor (DAA).[26] An increase in size is marked by the appearance of three-dimensional central cage forms with one or more four-coordinated core molecules in the interior. The simplest of the four-coordinated structures of the tetrahedral type is the pentamer C_2 (which is not the global minimum for pentamer) and the cluster $n = 12$, which contain four-coordinated water molecules of the double donor−double acceptor (DDAA) type.[26−29] This type of molecules is the main component of a crystal-like tetrahedral bond of ice *Ih* and ice *Ic* corresponding to the nearly perfect three-dimensional hydrogen-bonded network and also the main component of clusters. According to our results on water clusters[24] the ^{17}O shielding constants decreases as the ring size increases in clusters. These changes are dependent on ligand environment. We found a very large changes of $\sigma(^{17}O)$ within the four-coordinated oxygen DDAA type atom of −34.8 and −76.2 ppm for $n = 5$ and $n = 17$ clusters, respectively.[24]

This paper on a methane guest molecule in CHs is a continuation of our previous calculation study of NMR parameters in water clusters. Experimental NMR studies of the chemical shifts and dynamics of many guest molecules in CH have been published.[18,21,30] It has been demonstrated that ^{13}C NMR can distinguish methane in all cages found in the known types of structures;[13] for example, two separate peaks for ^{13}C chemical shifts of guest methane molecules (−3.6 and −5.9 ppm in a magic-angle spinning NMR measurement)[31,32] shows for two types of methane molecules within the solid hydrate. These signals were assigned to molecules entrapped in cages 5^{12} and $5^{12}6^2$, respectively.[31,32] The effect of the shape of the methane hydrate crystal on the ^{13}C chemical shift has been investigated by DFT method.[33] It has been found that the radius of the CH correlates with the ^{13}C chemical shifts. The calculations of the chemical shifts of xenon in sI and sII CH show that the environment cage affects the shifts of the Xe guest,[34] while H_2 guest molecules in the small and large cages cannot be distinguished.[21]

In this paper calculations of the methane and water molecule NMR chemical shifts and SSCCs in small and large cages are presented. The object of this study is to advance the understanding of the relation between NMR parameters and structure of the cage. Such a study offers a unique point for viewing the spectroscopic consequences of the effects of methane and water molecules binding to and between particular sites.

The cages may be perceived both simply as clusters of methane interacting with water molecules and as models of real methane CHs. When they are seen as clusters the analysis of our results is straightforward. In real crystals almost all water molecules are four coordinated (of the DDAA type), while in our models all water molecules are three coordinated (of the DAA and DDA types). This fact as well as the influence of external cages, present in the crystal structure of real CHs, should be considered. However, it was found recently that the presence of external cages influences NMR parameters negligibly.[33] Therefore, the conclusions drawn from our results can then be trusted and treated as representing crystalline structures.

The structure of this paper is as follows: first, in section II, the method employed for geometry optimization and the calculations of nuclear shielding and SSCCs are described. Next, in section III, the results of calculations of the NMR shielding and coupling constants are reported. Finally, a brief summary is presented in section IV.

II. COMPUTATIONAL DETAILS

Representation of the CH Structure. In this paper we treat two examples of CHs: the small cage 5^{12}, with 20 water molecules in 12 pentagonal faces, and the large one, $5^{12}6^2$ cage having 24 water molecules and two additional hexagonal faces. These two structures are shown in Figure 1. F1

Geometry Optimization. Structures used for the calculations were based on neutronographic data.[4] Initial arrangement of network of hydrogen bonds between water molecules was chosen according to Bernal and Fowler[35] ice rules as applied to polyhedral water clusters (PWC).[36] During most of the optimizations several rearrangements of this network were observed.

The structures of the cages were optimized by means of density-functional theory (DFT), using the hybrid three-parameter Becke−Lee−Yang−Parr (B3LYP) functional[37,38] with the basis set aug-cc-pVDZ.[39] At each stationary point located for all the clusters, a vibrational study was carried out in order to confirm whether it corresponds to a minimum on the potential energy surface. In the geometry optimizations (very tight option), no counterpoise corrections were made for the basis set superposition error. Previously, the DFT method was used to study small and large structures at DFT/B3LYP[40] and DFT/X3LYP,[41] respectively. We used the Gaussian 03 program[42] for the optimization of the structures.

As we have mentioned, PWCs are characterized by the fact that every water molecule forms 3 hydrogen bonds. Half of water molecules act as a double donor and single acceptor of hydrogen bond (DDA), while the rest of the water molecules act as a double acceptor and single donor of the hydrogen bond (DAA). Water molecules of the DDA type have a lone electron pair not involved in hydrogen bonding, while those of the DAA type have one OH bond not forming hydrogen bond, called a dangling OH bond. The total number of hydrogen bonds in a structure is equal to $3n/2$, and the number of dangling hydrogens is equal to $n/2$ (n is the number of water molecules). It is important to note that in real crystal the number of dangling hydrogens is rather small as they are present only in defects of the network. In studied systems there was one Bjerrum L-defect[43] present, namely, in the $5^{12}6^2$ cage one proton is turned toward methane molecule, and the corresponding hydrogen bond with neighboring water molecule is therefore weakened.

Calculations of the NMR Shielding Constants and SSCCs. The accurate determination of NMR parameters is a challenging

dx.doi.org/10.1021/jp110587x |J. Phys. Chem. A XXXX, XXX, 000–000

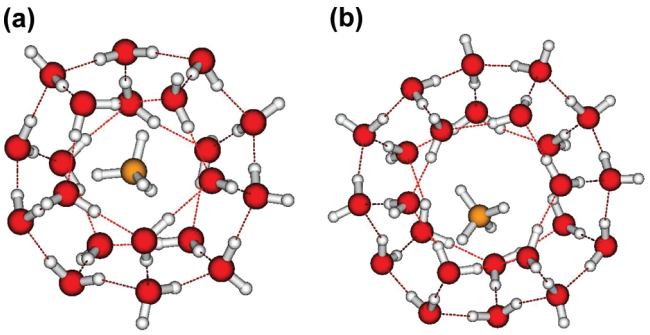

Figure 1. Structures of cages 5^{12} (a) and $5^{12}6^2$ (b) with enclathrated methane.

task requiring a high-level treatment of electron correlation and proper basis set, as many studies have shown previously.[22,23] Many-body perturbation theory (MBPT), coupled clusters with singles and doubles (CCSD), and multiconfigurational self-consistent field results are in agreement with the experimental data for many molecules, for example, for simple hydrides. However, the same does not hold for molecules with strong electron correlation effects (for example molecules containing the lone pairs or multiple bonds). The shielding constants of ^{17}O in water molecule belong to this group.[22,44] Since the MBPT approach for NMR chemical shift calculations is expensive, there is a growing interest in alternatives to shielding constants calculations. DFT provides such an alternative by inclusion of correlation effects in an approximate manner with modest computational costs. This is now the accepted method for studying large molecules with non-negligible correlation effects, even though this method has its own shortcomings.[22]

In this paper the calculations of the NMR shielding constants (SC) and indirect SSCC were carried out by using of the inexpensive DFT (with B3LYP functional). This method made it possible to carry out calculations for the CHs. London orbitals GIAO (gauge-independent atomic orbitals)[45] were used in shielding constants to ensure the gauge−origin independence.

The choice of basis set in calculations of complexation-induced changes in SCs and SSCCs is difficult, since the basis set should be appropriate for both: the calculations of the NMR parameters and the interaction energy. The indirect nuclear SSCCs depend critically on the molecular electronic structure close to the coupled nuclei, while diffuse functions are essential for the proper description of hydrogen bonds. As a consequence, the calculations of SSCCs for interacting systems require both a good description of core orbitals and the presence of diffuse orbitals. This problem was studied in our previous paper for water dimer.[46,47] Therefore, according to the conclusion of our study,[46] and because our purpose is to study the relative NMR parameters in the clathrates for practical considerations, we used the HuzIII-su3 basis set.[48] The SCs and SSCCs calculations were carried out with the DALTON program.[49]

III. RESULTS AND DISCUSSION

Shielding Constants. Methane. Shielding constants and anisotropies for protons and carbon nuclei of methane inside the clathrates are presented in Table 1 (for more detailed data for both cages, see Table 1 of Supporting Information), together with experimental values of $\sigma(^{13}C)$ and $\sigma(^{1}H)$ for gaseous methane, cited from Antusek et al.[50] According to our calculations, the shifts in the ^{13}C isotropic constants upon complexation, with respect to the methane monomer, are equal to 6.02 and 4.75 ppm for the 5^{12} and $5^{12}6^2$ cages, respectively, while the shifts for ^{1}H are 0.55 and 0.57 ppm. The carbon atom is thus more affected and deshielded by the methane−water cage interaction than methane's hydrogens. The ^{13}C shielding is increasing with the increasing number of water molecules, i.e., with the increasing cavity size, toward the value of gaseous methane's carbon. The para- and diamagnetic components of shielding constants are both systematically greater in the case of $5^{12}6^2$ cage for all methane atoms, but the differences are of the same magnitude and cancel each other (see Table 1 of Supporting Information).

Table 1. Shielding Constants ^{17}O, ^{13}C, and ^{1}H and Their Anisotropy for Water and Methane Molecules at 5^{12} and $5^{12}6^2$ Cages (Optimized at B3LYP/aug-cc-pVDZ, NMR at B3LYP/HuzIII-su3)[a,b]

		5^{12}		$5^{12}6^2$	
molecule	atom	σ [ppm]	anisotropy	σ [ppm]	anisotropy
methane	C	182.01	−1.51	183.28	1.50
	H	31.10	9.31	31.08	9.22
water	DAA O	289.18	41.18	288.75	42.62
	DDA O	288.95	19.28	290.78	15.16
	DAA H	23.71	32.93	23.73	33.31
	DAA H*	30.52	19.41	30.51	18.90
	DDA H	26.61	28.24	26.73	28.60

[a] Values for monomers (optimized at B3LYP/HuzIII-su3, all in ppm): $\sigma^{C}_{methane}$ = 188.03, anisotropy = −0.03; $\sigma^{H}_{methane}$ = 31.65, anisotropy = 9.10; σ^{O}_{water} = 325.00, anisotropy = 51.48; σ^{H}_{water} = 31.34, anisotropy = 18.90. Experimental values from ref 50: $\sigma^{C}_{methane}$ = 195.02; $\sigma^{H}_{methane}$ = 30.61; σ^{O}_{water} = 322.81; σ^{H}_{water} = 30.05. [b] Asterisk denotes dangling hydrogens.

Let us now compare these values with the experimental data mentioned in the Introduction. Three resonance lines with the chemical shifts of −3.6, −5.9, and −10.3 ppm for the 5^{12} and $5^{12}6^2$ cages and gas-phase methane, respectively, were measured.[31,32] Thus, a larger shift of the ^{13}C shielding constant with respect to methane was found for the 5^{12} cage (6.7 ppm) than for the $5^{12}6^2$ cage (4.4 ppm). These values are close to the differences calculated by us: 6.02 for 5^{12} and 4.75 ppm for $5^{12}6^2$ cages. Therefore, based on the observation of the complexation-induced shifts in ^{13}C shielding constants of the central carbon atom, one can discriminate between two cages.

An important comment on the comparison of experimental and calculated chemical shifts should be added here. It was shown that the methane molecule inside both cavities behaves as a free rotor in temperatures higher than a few Kelvin.[51,52] Influence of the rotation on SCs is thus similar in both cases. It was also shown that vibrations of methane are affected by the presence of water network,[53] so their influence on shielding is different for enclathrated and gaseous molecules. Thus experimental chemical shifts of enclathrated methane with respect to gaseous methane are describing influence of both the change in electronic density around nuclei and change in vibrational characteristics. In our calculations we have obtained SCs for static systems, i.e., without corrections for rovibrational effects, therefore only the electronic density changes arising from enclathration affect our SCs values.

Water Molecules. First, let us discuss the induced shifts in the ^{17}O shielding constants in CHs. Both shielding constants and anisotropies for oxygen nuclei are presented in Table 1. Through this paper we shall use the symbol $\Delta\sigma$ for the environment-induced

dx.doi.org/10.1021/jp110587x |J. Phys. Chem. A XXXX, XXX, 000–000

changes in the shielding constants and not, as usual, for the shielding anisotropy. The para- and diamagnetic components of shielding constants are tabulated at Tables 2 and 3 of Supporting Information. The experimental absolute shielding constant determined by Wasylishen and Bryce is 323.6 ± 0.6 ppm.[54] The gas-to-liquid experimental chemical shifts for water are known to be −36.1 ppm for oxygen and −4.26 ppm for protons.[55]

Taking a single water molecule from the monomeric state as a reference state for gas (calculated $\sigma(^{17}O) = 325.0$ ppm), the oxygen shielding constants decrease at both type of water molecules, DDA and DAA, interacting with methane and other water molecules in the two investigated cages. The changes of σ are −35.8 ppm (DAA) and −36.1 ppm (DDA) in the cage 5^{12}, and in the cage $5^{12}6^2$ these numbers are −36.2 (DAA) and −34.22 ppm (DDA). Thus, the interaction-induced shifts of oxygen nuclei are dependent on environment, although the difference between two cages are small. In the case of DDA oxygens, however, the average anisotropies differ by about 30%, and that can serve as a discriminating factor between two cages.

The changes of the ^1H shielding constants depend mainly on whether the hydrogen atom is involved in a hydrogen bond or not. The $\Delta\sigma(^1H)$ of the proton involved in a hydrogen bond decreases by −7.63 (DAA) or by −4.73 ppm (DDA) in the case of the 5^{12} cage and is almost the same value in the case of $5^{12}6^2$. The change of the proton shielding constants in the dangling hydrogens are less substantial (ca. −0.8 ppm for both cages). It was found by Cybulski et al.[24] that the values of shifts $\Delta\sigma(^1H)$ correlate with the O−H distances and with the inverse of the intermolecular H···O and O···O distances. This observation is true for both CHs (for $5^{12}6^2$ cage $R(OH) = 0.977$ for DDA, while it is 0.991 Å for DAA and $R(O\cdots O) = 2.868$ for DDA, while it is 2.750 Å for DAA). The gas-to-liquid experimental chemical shifts for proton are known to be −4.26 ppm.[55] Thus, it seems, presented calculated values are reasonable. On the other hand, anisotropies are different for each type of hydrogen atoms but independent of the cage type.

SSCCs. Intramolecular SSCCs $^1J_{CH}$ and $^2J_{HH}$ in Methane and $^1J_{OH}$, $^2J_{HH}$ in Water Molecules. The calculated SSCCs for methane molecules are collected in Table 2 (see Table 4 of Supporting Information) together with experimental[56] and theoretical data. The values of $^1J_{CH}$ and $^2J_{HH}$ are in agreement with the previously calculated couplings (123.86 and −14.3 Hz[22]) at the CCSDPPA level, which were claimed to be the most reliable ones. According to our calculations, the shifts in the $^1J_{CH}$ upon complexation (with respect to the methane monomer) are equal to −1.04 and −1.23 Hz for 5^{12} and $5^{12}6^2$ cages, respectively, while the shifts in the $^2J_{HH}$ is 0.07 and 0.05 Hz for both cages, respectively. The total values of both SSCCs and the values of corresponding components are close for two cages. The predominant component is FC term, which is responsible for about 99% of the value of the coupling constants. Other components are very small and does not affect the final value. The differences between bond lengths are very small, but they have an visible effect on the FC value (see Table 4 of Supporting Information).

The changes of the calculated $^1J_{OH}$ and $^2J_{HH}$ coupling constants due to formation of the CH are presented in Table 2 (see Tables 5 and 6 of Supporting Information for detailed data). First, we discuss the effects caused by the formation of hydrogen bonding on $^1J_{OH}$. There are three different types of OH bonds present in both cages. Two of them are present in DAA water molecules, namely, OH bonds involved in H bonding and not involved in H bonding (having dangling hydrogens), which SSCCs are denoted $^1J_{OH}^{DAA}$ and $^1J_{OH^*}^{DAA}$, respectively. The third category are OH bonds of DDA water molecules, both involved in H-bonding, with SSCCs denoted $^1J_{OH}^{DDA}$. The formation of the hydrogen bond in 5^{12} cage influences strongest the $^1J_{OH}^{DAA}$ by −7.55 Hz (from −76.04 in the monomer to −83.59 Hz). The changes of $^1J_{OH^*}^{DAA}$ and $^1J_{OH}^{DAA}$ are slightly smaller (−6.96 and −6.84 Hz, respectively). Similar changes can be found for cage $5^{12}6^2$ (−6.39, −7.75, and −6.69 Hz, respectively, for $^1J_{OH}^{DAA}$, $^1J_{OH^*}^{DAA}$ and $^1J_{OH}^{DAA}$). Thus, independent of the type of water molecule, the hydrogen-bonding formation appears to increase the absolute value of $^1J_{OH}$. What are the changes of the individual contributions to the SSCC? The values, presented in Table 6 of Supporting Information, are dominated by a Fermi contact (FC) term giving 88% of total value. Among other three components only Pauli spin-orbit (PSO) is of importance, adding 11% in both cases, while diamagnetic spin-orbit (DSO) and spin-dipole (SD) influence on the final value of coupling together on average is less than 1%.

Table 2. Intramolecular $^XJ_{YZ}$ [Hz] in Methane and Water Molecules for 5^{12} and $5^{12}6^2$ Cages[a,b]

molecule	coupling	5^{12}	$5^{12}6^2$
CH_4	$^1J_{CH}$	134.18	134.37
	$^2J_{HH}$	−13.42	−13.44
H_2O	$^2J_{HH}^{DAA}$	−7.65	−7.66
	$^2J_{HH}^{DDA}$	−8.21	−8.04
	$^1J_{OH}^{DAA^*}$	−83.00	−83.41
	$^1J_{OH}^{DAA}$	−83.59	−83.79
	$^1J_{OH}^{DDA}$	−82.88	−83.73
	$^1J_{OH}^{average}$	−83.09	−83.66

[a] Values for monomers (optimized at B3LYP/HuzIII-su3, all in [Hz]); CH_4, $^1J_{CH} = 133.14$ and $^2J_{HH} = -13.49$; H_2O, $^1J_{OH} = -76.04$ and $^2J_{HH} = -7.72$. Experimental values:[56,59,60] CH_4, $^1J_{CH} = 125.31$ and $^2J_{HH} = -12.4$; H_2O, $^1J_{OH} = 80.6$. [b] Asterisk denotes dangling water hydrogens.

The range of the intramolecular OH bond lengths is 0.96−1.02 Å, and it is possible to catch some tendencies of the changes of SSCCs with bond lengths. The results for the $5^{12}6^2$ cage are depicted in parts a−c of Figure 2, while Figure 1 of Supporting Information presents the results for the 5^{12} cage. By analysis of these figures, we do not observe any smooth dependence of the calculated $^1J_{OH}$. However, we can recognize some trends. Like in water clusters, this parameter increases (in absolute values) with the increase of the O−H intramolecular distance. The largest term FC determines the behavior of the total coupling. The standard deviation is twice greater for the $5^{12}6^2$ cage in comparison to the 5^{12} cage. In the case of 5^{12}, interpretation of the plots is much clearer—total J value remains constant, while absolute value of FC component is slightly rising with distance. The changes in the three other components values are the same for both cages; they behave more regularly.

A second intramolecular coupling constant, which could be interesting for the characterization of CH is $^2J_{HH}$ (see Table 2 and Table 5 of Supporting Information for details, Figure 3 for $5^{12}6^2$, and Figure 2 of Supporting Information for 5^{12}). In water dimer this parameter increases (in absolute value) after formation of the hydrogen bond.[46] Similar trends are noticed for CH: in the 5^{12} cage hydrogen bond induced change is −0.49, while in the $5^{12}6^2$ cage it is −0.32 Hz. Average values of these coupling constants are the same for both cages. The FC components have the greatest values, which are of the same order of magnitude as the total coupling constants. Absolute value of PSO (which is about 70% of total SSCC) is slightly greater than DSO, so being of opposite signs they

dx.doi.org/10.1021/jp110587x | J. Phys. Chem. A XXXX, XXX, 000–000

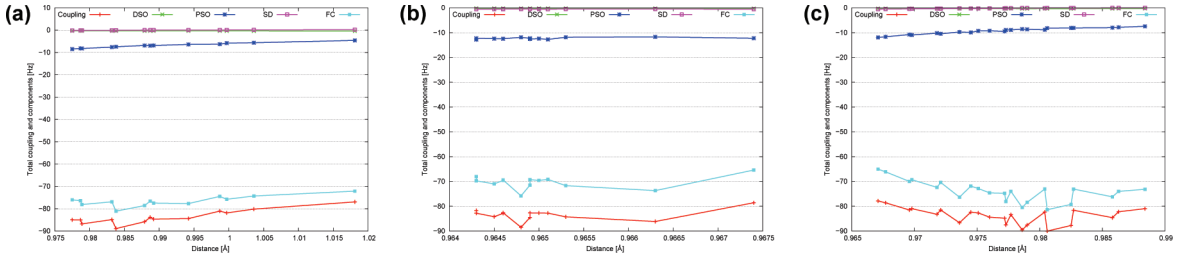

Figure 2. Intramolecular $^{1}J_{OH}$ and its components (FC, SD, PSO and DSO) as a function of intramolecular O−H distance for cage $5^{12}6^{2}$ in (a) DAA water molecules, hydrogen is H-bond involved, (b) DAA water molecules, dangling hydrogen H*, and (c) DDA water molecules.

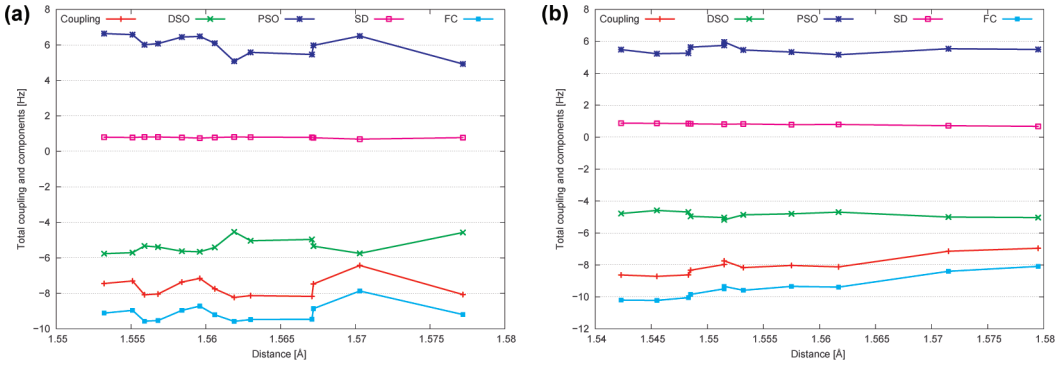

Figure 3. Intramolecular $^{2}J_{HH}$ and its components (FC, SD, PSO, and DSO) as a function of the H···H distance for the $5^{12}6^{2}$ cage in (a) DAA water molecules and (b) DDA water molecules.

mostly cancel each other. The SD component is 10% of the final coupling constant value.

Intermolecular $^{1h}J_{OH}$, $^{3h}J_{OH}$, $^{2h}J_{OO}$, and $^{1h}J_{HO}^{methane-water}$ Coupling Constants. It is possible to distinguish several types of intermolecular SSCCs in the cages. Water's oxygens couple with neighboring water's hydrogens and two types of those H-bond transmitted couplings will be characterized below, namely, $^{1h}J_{OH}$ and $^{3h}J_{OH}$. The next important group of intermolecular H-bond transmitted SSCCs is $^{2h}J_{OO}$, between oxygen atoms of neighboring water molecules. The third category of SSCCs consists of couplings between methane's hydrogens and water's oxygens $^{1h}J_{HO}^{methane-water}$.

First, let us discuss the intermolecular O···O coupling constants between oxygen atoms of neighboring water molecules $^{2h}J_{OO}$. The results are presented in Table 3 and Table 7 of Supporting Information. It is possible to divide all the O···O pairs into three categories, depending on the coordination of water molecules involved, namely, DAA−DAA, DAA−DDA, and DDA−DDA. Table 3 contains also the average values of SSCCs. It is worth noticing that the average values of the $^{2h}J_{OO}$ tend to be larger in the $5^{12}6^{2}$ cage than in the smaller one. Values of the average coupling constants show exponential decay with the R(O···O), which is depicted in Figure 4 for $5^{12}6^{2}$ and Figure 3 of Supporting Information for 5^{12}. The intermolecular SSCCs between two oxygen nuclei transmitted through two bonds covers the range between 3.04 and 5.05 Hz (Table 3). The largest and the smallest values are observed for the shortest (2.774 Å) and longest (2.834 Å) intermolecular O···O distances, respectively. In all three cases, DAA−DAA, DAA−DDA, and DDA−DDA pairs, the changes in the total couplings are determined by the changes in the FC term, which decreases in an exponential manner, similarly as for small water clusters.[57] The DSO term for the whole distance range is close to zero (see Figure 4), while SD and PSO depend linearly on O···O distance.

Table 3. Intermolecular $^{xh}J_{YZ}$ [Hz] at B3LYP/HuzIII-su3 for Water Molecules in the 5^{12} and $5^{12}6^{2}$ Cages

	5^{12}		$5^{12}6^{2}$	
coupling type	r [Å]	J [Hz]	r [Å]	J [Hz]
$^{2h}J_{OO}^{DAA-DAA}$	2.774	5.05	2.784	4.54
$^{2h}J_{OO}^{DDA-DDA}$	2.775	4.05	2.798	3.54
$^{2h}J_{OO}^{DDA-DAA}$	2.834	3.04	2.798	3.88
$^{2h}J_{OO}^{average}$	2.807	3.74	2.794	3.95
$^{1h}J_{OH}^{DAA-DAA}$	1.789	6.86	1.834	6.36
$^{3h}J_{OH}^{DAA-DAA}$	3.226	−0.38	3.275	−0.17
$^{1h}J_{OH}^{DDA-DDA}$	1.791	6.72	1.843	6.32
$^{3h}J_{OH}^{DDA-DDA}$	3.107	0.55	3.139	0.54
$^{1h}J_{OH}^{(O)DDA-(H)DAA}$	1.683	7.73	1.629	8.00
$^{3h}J_{OH}^{(O)DDA-(H)DAA}$	3.118	0.73	3.122	0.57
$^{1h}J_{OH}^{(O)DAA-(H)DDA}$	1.952	5.08	1.928	5.34
$^{3h}J_{OH}^{(O)DAA-(H)DDA}$	3.138	0.60	3.142	0.56

For the DAA−DDA pairs (1b) general features are the same as for averages. The exponential dependence of coupling constants, FC, PSO, and SD components on interatomic separation is even more evident. On the plot the for $5^{12}6^{2}$ cage there is one value displaced from the exponential dependence (at 2.76 Å). One of oxygens involved in this coupling belongs to defected water, interacting via its hydrogen with the methane inside the cage. This irregularity does not invalidate the general conclusion then.

Coupling constants between DAA−DAA in both cages are greater by ca. 1 Hz than average values. The range of distances O···O is smaller for DAA−DAA pairs (2.65−2.86 Å) than for DAA−DDA and DDA−DDA. This may be the reason why the

dx.doi.org/10.1021/jp110587x |J. Phys. Chem. A XXXX, XXX, 000–000

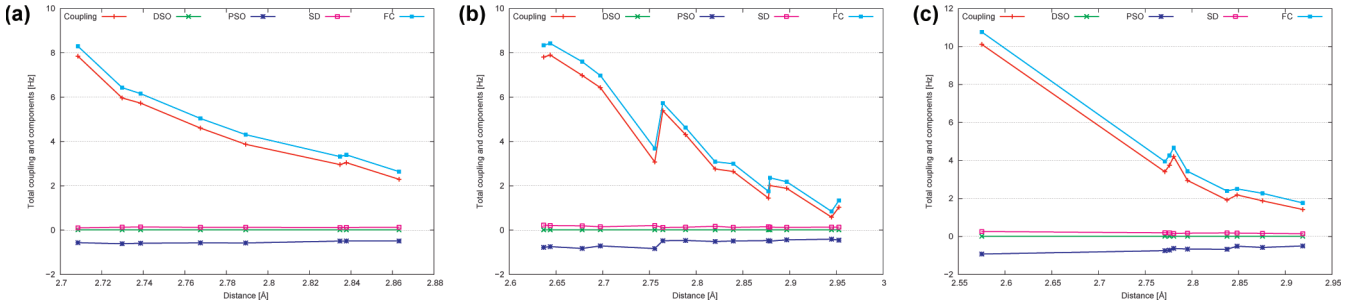

Figure 4. Intermolecular $^{2h}J_{OO}$ and its components (FC, SD, PSO and DSO) as a function of the O···O distance for cage $5^{12}6^2$ for (a) DAA−DAA water molecules, (b) DDA−DAA water molecules, and (c) DDA−DDA water molecules.

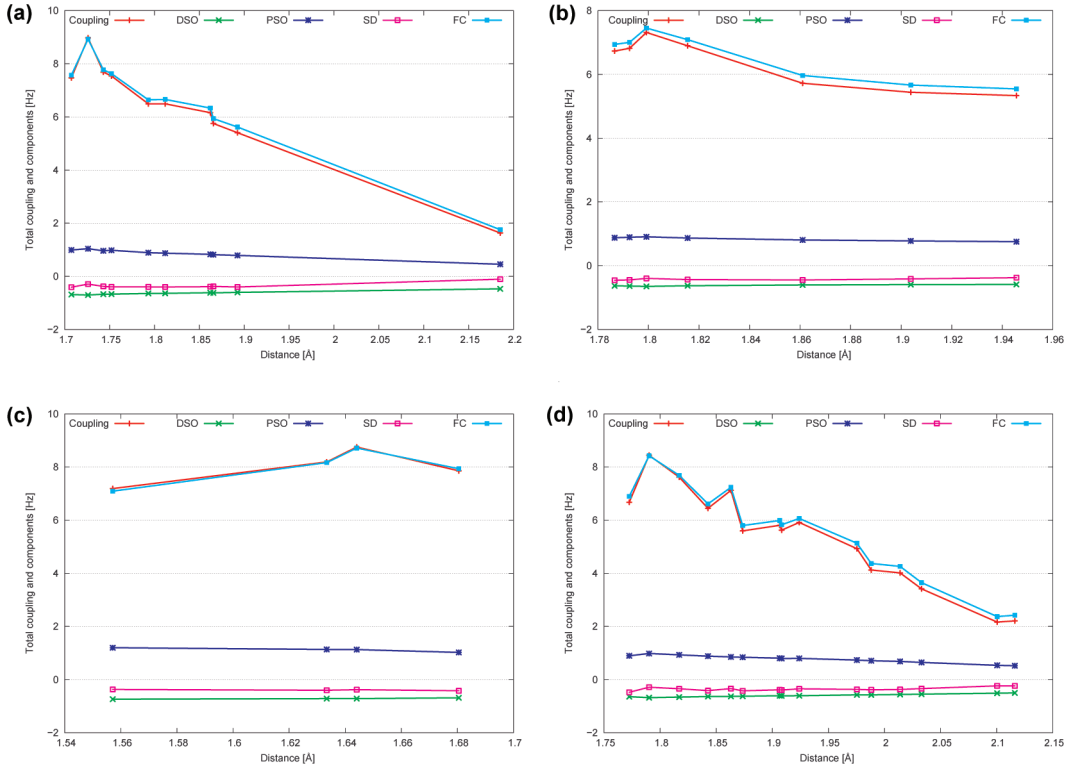

Figure 5. Intermolecular $^{1h}J_{OH}$ and its components (FC, SD, PSO, and DSO) as a function of the O···H distance for cage $5^{12}6^2$ for (a) DAA−DAA water molecules, (b) DDA−DDA water molecules, (c) DDA−DAA water molecules, where DDA is a proton acceptor from DAA, and (d) DAA−DDA water molecules, where DAA is a proton acceptor from DDA.

changes of SD and PSO terms do not show clear tendencies with growing interoxygen separation.

DDA−DDA coupling constants are very close to average values for all types of water pairs. The linear dependence of coupling constants and distinct components on internuclear distance is preserved. The shape of the curves for FC term and the values of coupling constants resembles exponential decay.

Now we would like to discuss two other types of hydrogen bonds transmitted coupling constants: $^{1h}J_{OH}$ and $^{3h}J_{OH}$. First coupling is observed between H-bonded oxygen and hydrogen nuclei and is denoted $^{1h}J_{OH}$, while the other couples oxygen with the second proton of neighboring water; therefore the coupling is transferred through 3 bonds and is denoted $^{3h}J_{OH}$. Those two types of couplings could easily be differentiated on the base of the distance between coupling atoms: if oxygen is not H-bonded with relevant hydrogen, they are separated by more than 2.98 Å, while for H-bonded maximum distance is not greater than 2.10 Å. In the following sections this distinction will be combined with the former one based on the type of water molecule H-bonding pattern. There are three groups that can be distinguished, namely, DAA−DAA, DDA−DDA, and DDA−DAA pairs.

The average $^{1h}J_{OH}$ transmitted through hydrogen bond H···O are substantial, as shown in Table 1, Figure 5 for the $5^{12}6^2$ cage, Figure 4 of Supporting Information for the 5^{12} cage, and Table 8 of Supporting Information. They are within the range of 5.1−8.0 Hz. These couplings are dominated by the FC term; the three remaining terms are nearly negligible. The spin−orbit terms DSO and PSO are of similar magnitude but opposite sign; their sum does not contribute significantly to the total coupling. The average intermolecular bond lengths H···O vary from 1.68 to 1.95 Å for the 5^{12} cage and from 1.63 to 1.93 Å for the $5^{12}6^2$ cage.

Table 3 presents also the $^{3h}J_{OH}$ SSCCs. These couplings, despite average internuclear oxygen-proton nuclei distance of more than 3 Å, are for both cages of the order of 0.5 Hz. This can be attributed

dx.doi.org/10.1021/jp110587x |J. Phys. Chem. A XXXX, XXX, 000–000

to the strength of hydrogen bonds between neighboring water molecules, which elevates the value of the coupling.

Now we would like to discuss the dependence of the intermolecular $^{1h}J_{OH}$ constants on the H···O intermolecular separation for three groups of interacting water molecules: DAA−DAA (Figure 5a), DDA−DDA (Figure 5b), (O)DDA−(H)DAA (Figure 5c), and (O)DAA−(H)DDA (Figure 5d). First we will analyze the case when both H and O nulei belong to DAA or both to DDA water. These two types of couplings are characterized by similar average values of SSCCs transmitted through hydrogen bond of similar length. The $^{1h}J_{OH}$ coupling increases with the decrease of the H···O intermolecular distance (Figure 5 for $5^{12}6^2$ cage). There is a linear dependence of FC and coupling constant values−they are both linearly decreasing with distance for both cages (see also Figure 4 of Supporting Information for the 5^{12} cage).

The next category is: H and O belong to different types of water molecules. This group can be split into two subgroups, one for the proton belonging to DDA water and oxygen nucleus to DAA water and the second for the opposite situation. When the donor proton belongs to DAA water (Figure 5c) the average coupling constant for both cages is around 8.0 Hz with average distance around 1.65 Å. The average contributions from FC equals final total coupling value, while for DSO, PSO, and SD terms are −9, 14, and −5%, respectively.

In the opposite situation (depicted at Figure 5d), the distance H···O is ca. 1.94 Å, and the average coupling constant $^{1h}J_{OH}$ for both cages is thus smaller, between 5.0 and 5.5 Hz. By analysis of these changes, we observed a decay of $^{1h}J_{OH}$ with the intermolecular H···O distance, contrary to the changes in previous data (parts a and b of Figure 5). The contributions of different components are −11, 15, −7, and 103% for DSO, PSO, SD, and FC, respectively, so they are by 1−3% greater than in former case.

That data suggests that the hydrogen bond between DDA-type water molecules acting as a proton acceptor from DAA-type water molecules are stronger than one formed by DAA water acting as acceptor for DDA water proton.

The last category of intermolecular SSCCs we want to comment on is the coupling between methane's hydrogens and water's oxygens $^{1h}J_{HO}^{methane-water}$. Most of them are of the order of 0.1 Hz (only one coupling reaches 0.6 Hz) as the distance between coupled atoms exceeds 3 Å. The energy of those interactions was estimated at MP2 level[58] as a small one, which corresponds to the small values of couplings. All other types of intermolecular SSCCs are very small.

Recently, considerable progress has been made in employing SSCCs as parameters describing hydrogen bonds. The range of intermolecular J-coupling constants for CHs is small; however, a developments in experimental technique will probably made them measurable in the future.

IV. CONCLUSIONS

DFT/B3LYP calculations have been performed to obtain ^{17}O, ^{1}H, and ^{13}C shielding constants and O−O, O−H, and C−H intra- and intermolecular SSCCs for two models of methane in the cages 5^{12} and $5^{12}6^2$ of sI CH. Our analysis of the calculated parameters is focused mainly on their presumed correlation with the topology of the cages and types of hydrogen bonding in water molecules. The results of these calculations support the following statements.

(1) The ^{13}C shielding is increasing with the increasing cavity size, toward the value of gaseous methane's carbon. It is in agreement with the experimental findings that ^{13}C NMR can distinguish methane in cages found in known types of structures.

(2) The ^{17}O shielding constants decreases in both cages. The changes of σ are −35.8 ppm for DAA-type water molecules and −36.1 ppm for DDA molecules in the 5^{12} cage, while in the $5^{12}6^2$ cage these numbers are −36.2 (DAA) and −34.2 ppm (DDA). Thus, the interaction-induced shifts of oxygen nuclei are dependent on environment, although the difference between two cages are small. Let us mention that the gas-to-liquid experimental chemical shifts for water are very close and are known to be −36.1 ppm for oxygen.

(3) The complexation-induced changes in the intramolecular proton−proton coupling constants $^{2}J_{HH}$ and the proton-oxygen $^{1}J_{OH}$ do not vary significantly in DAA and DDA type of water in both cages. Therefore, independent of the type of water molecule, the hydrogen-bonding formation appears to increase the absolute values of $^{1}J_{OH}$ and $^{2}J_{HH}$.

(4) On the other hand the intermolecular $^{1h}J_{OH}$ transmitted through the hydrogen bond H···O is substantial. The increase of their values is connected with the elongation of the intramolecular O−H bond and the shortening of the intermolecular O···O distance. When the proton belongs to DAA water the average coupling constant for both cages is around 8.0 Hz with average distance around 1.65 Å. In the opposite situation, the distance H···O is around 1.94 Å, and the average coupling constant $^{1h}J_{OH}$ for both cages is thus smaller, between 5.0 and 5.5 Hz. These data suggests: hydrogen bond between DDA-type water molecules acting as a proton acceptor from DAA-type water molecules is stronger than one formed by DAA type water molecules acting as proton acceptor from DDA water.

■ ASSOCIATED CONTENT

Supporting Information. Figures depicting intramolecular $^{1}J_{OH}$ and its components (FC, SD, PSO, and DSO) as a function of the O−H distance for cage 5^{12}, intramolecular $^{2}J_{HH}$ and its components (FC, SD, PSO, and DSO) as a function of the H−H distance for cage 5^{12}, intermolecular $^{2h}J_{OO}$ and its components (FC, SD, PSO, and DSO) as a function of the O−O distance for cage 5^{12}, and intermolecular $^{1h}J_{OH}$ and its components (FC, SD, PSO, and DSO) as a function of the O−H distance for cage 5^{12}. Tables with shielding constants and anisotropy values for all components of both cages. This material is available free of charge via the Internet at http://pubs.acs.org.

■ AUTHOR INFORMATION

Corresponding Author

*E-mail: sadlej@chem.uw.edu.pl.

■ ACKNOWLEDGMENT

We would like to thank MSc Jan Stanek, who helped us in obtaining structures for the calculations. The Foundation for Polish Science is acknowledged for financial support.

■ REFERENCES

(1) Chihaia, V.; Adams, S.; Kuhs, W. F. *Chem. Phys.* **2004**, *297*, 271–287.

(2) Sloan, E. D. *Nature* **2003**, *426*, 353–363.

(3) Ripmeester, J. A.; Tse, J. S.; Ratcliffe, C. I.; Powell, B. M. *Nature* **1987**, *325*, 135–136.
(4) Sloan, E. D.; Koh, C. A. *Clathrate Hydrates of Natural Gases*, 3rd ed.; CRC Press: New York, 2008.
(5) McCarthy, V. N.; Jordan, K. D. *Chem. Phys. Lett.* **2006**, *429*, 166–168.
(6) Ripmeester, J. A.; Ding, L.; Klug, D. D. *J. Phys. Chem.* **1996**, *100*, 13330–13332.
(7) Alavi, S.; Susilo, R.; Ripmeester, J. A. *J. Chem. Phys.* **2009**, *130*, 174501.
(8) Susilo, R.; Alavi, S.; Ripmeester, J. A.; Englezos, P. *J. Chem. Phys.* **2008**, *128*, 194505.
(9) Buch, V.; Devlin, J. P.; Monreal, I. A.; Jagoda-Cwiklik, B.; Uras-Aytemiz, N.; Cwiklik, L. *Phys. Chem. Chem. Phys.* **2009**, *11*, 10245–10265.
(10) Monreal, I. A.; Cwiklik, L.; Jagoda-Cwiklik, B.; Devlin, J. P. *J. Phys. Chem. Lett.* **2010**, *1*, 290–294.
(11) Walsh, M. R.; Koh, C. A.; Sloan, E. D.; Sum, A. K.; Wu, D. T. *Science* **2009**, *326*, 1095–1098.
(12) Nakayama, T.; Koga, K.; Tanaka, H. *J. Chem. Phys.* **2009**, *131*, 214506.
(13) Myshakin, E. M.; Jiang, H.; Warzinski, R. P.; Jordan, K. D. *J. Phys. Chem. A* **2009**, *113*, 1913–1921.
(14) Chou, I.-M.; Sharma, A.; Burruss, R. C.; Shu, J.; Mao, H.-k.; Hemley, R. J.; Goncharov, A. F.; Stern, L. A.; Kirby, S. H. *Proc. Natl. Acad. Sci. U.S.A.* **2000**, *97*, 13484–13487.
(15) Ripmeester, J. A.; Ratcliffe, C. I. *J. Phys. Chem.* **1988**, *92*, 337–339.
(16) Shimizu, H.; Kumazaki, T.; Kume, T.; Sasaki, S. *J. Phys. Chem. B* **2002**, *106*, 30–33.
(17) Ida, T.; Mizuno, M.; Endo, K. *J. Comput. Chem.* **2002**, *23*, 1071–1075.
(18) Lee, H.; Seo, Y.; Seo, Y.-T.; Moudrakovski, I. L.; Ripmeester, J. A. *Angew. Chem., Int. Ed.* **2003**, *42*, 5048–5051.
(19) Hartke, B. *J. Chem. Phys.* **2009**, *130*, 024905.
(20) Bravo-Perez, G.; Cruz-Torres, A.; Romero-Martinez, A. *J. Phys. Chem. A* **2008**, *112*, 8737–8751.
(21) Alavi, S.; Ripmeester, J. A.; Klug, D. D. *J. Chem. Phys.* **2005**, *123*, 051107.
(22) Helgaker, T.; Jaszunski, M.; Ruud, K. *Chem. Rev.* **1999**, *99*, 293–352.
(23) Helgaker, T.; Jaszunski, M.; Pecul, M. *Prog. Nucl. Magn. Reson. Spectrosc.* **2008**, *53*, 249–268.
(24) Cybulski, H.; Sadlej, J. *Chem. Phys.* **2006**, *323*, 218–230.
(25) Pecul, M.; Lewandowski, J.; Sadlej, J. *Chem. Phys. Lett.* **2001**, *333*, 139–145.
(26) Buck, U.; Ettischer, I.; Melzer, M.; Buch, V.; Sadlej, J. *Phys. Rev. Lett.* **1998**, *80*, 2578–2581.
(27) Brudermann, J.; Melzer, M.; Buck, U.; Kazimirski, J. K.; Sadlej, J.; Buch, V. *J. Chem. Phys.* **1999**, *110*, 10649–10652.
(28) Sadlej, J.; Buch, V.; Kazimirski, J. K.; Buck, U. *J. Phys. Chem. A* **1999**, *103*, 4933–4947.
(29) Sadlej, J. *Chem. Phys. Lett.* **2001**, *333*, 485–492.
(30) Lee, H.; Lee, J.-w.; Kim, D. Y.; Park, J.; Seo, Y.-T.; Zeng, H.; Moudrakovski, I. L.; Ratcliffe, C. I.; Ripmeester, J. A. *Nature* **2005**, *434*, 743–746.
(31) Dec, S. F.; Bowler, K. E.; Stadterman, L. L.; Koh, C. A.; Sloan, E. D. *J. Am. Chem. Soc.* **2006**, *128*, 414–415.
(32) Gupta, A.; Dec, S. F.; Koh, C. A.; Sloan, E. D., Jr. *J. Phys. Chem. C* **2007**, *111*, 2341–2346.
(33) Terleczky, P.; Nyulaszi, L. *Chem. Phys. Lett.* **2010**, *488*, 168–172.
(34) Stueber, D.; Jameson, C. J. *J. Chem. Phys.* **2004**, *120*, 1560–1571.
(35) Bernal, J. D.; Fowler, R. H. *J. Chem. Phys.* **1933**, *1*, 515–548.
(36) Anick, D. J. *THEOCHEM* **2002**, *587*, 87–96.
(37) Becke, A. D. *J. Chem. Phys.* **1993**, *98*, 5648–5652.
(38) Lee, C.; Yang, W.; Parr, R. G. *Phys. Rev. B* **1988**, *37*, 785–789.
(39) T. H. Dunning, J. *J. Chem. Phys.* **1989**, *90*, 1007–1023.
(40) Estrin, D. A.; Paglieri, L.; Corongiu, G.; Clementi, E. *J. Phys. Chem.* **1996**, *100*, 8701–8711.
(41) Su, J. T.; Xu, X.; Goddard, W. A. *J. Phys. Chem. A* **2004**, *108*, 10518–10526.
(42) Frisch, M. J.; Trucks, G. W.; Schlegel, H. B.; Scuseria, G. E.; Robb, M. A.; Cheeseman, J. R.; Montgomery, J. A., Jr.; Vreven, T.; Kudin, K. N.; Burant, J. C.; Millam, J. M.; Iyengar, S. S.; Tomasi, J.; Barone, V.; Mennucci, B.; Cossi, M.; Scalmani, G.; Rega, N.; Petersson, G. A.; Nakatsuji, H.; Hada, M.; Ehara, M.; Toyota, K.; Fukuda, R.; Hasegawa, J.; Ishida, M.; Nakajima, T.; Honda, Y.; Kitao, O.; Nakai, H.; Klene, M.; Li, X.; Knox, J. E.; Hratchian, H. P.; Cross, J. B.; Bakken, V.; Adamo, C.; Jaramillo, J.; Gomperts, R.; Stratmann, R. E.; Yazyev, O.; Austin, A. J.; Cammi, R.; Pomelli, C.; Ochterski, J. W.; Ayala, P. Y.; Morokuma, K.; Voth, G. A.; Salvador, P.; Dannenberg, J. J.; Zakrzewski, V. G.; Dapprich, S.; Daniels, A. D.; Strain, M. C.; Farkas, O.; Malick, D. K.; Rabuck, A. D.; Raghavachari, K.; Foresman, J. B.; Ortiz, J. V.; Cui, Q.; Baboul, A. G.; Clifford, S.; Cioslowski, J.; Stefanov, B. B.; Liu, G.; Liashenko, A.; Piskorz, P.; Komaromi, I.; Martin, R. L.; Fox, D. J.; Keith, T.; Al-Laham, M. A.; Peng, C. Y.; Nanayakkara, A.; Challacombe, M.; Gill, P. M. W.; Johnson, B.; Chen, W.; Wong, M. W.; Gonzalez, C.; Pople, J. A. *Gaussian 03*, revision C.02; Gaussian, Inc.: Wallingford, CT, 2004.
(43) Bjerrum, N. *Mat. Fys. Medd.* **1951**, *27*, 1.
(44) Vaara, J.; Lounila, J.; Ruud, K.; Helgaker, T. *J. Chem. Phys.* **1998**, *109*, 8388–8397.
(45) London, F. W. *J. Phys. Rad.* **1937**, *8*, 397–409.
(46) Pecul, M.; Sadlej, J. *Chem. Phys. Lett.* **1999**, *308*, 486–494.
(47) Del Bene, J. E.; Elguero, J. *Mol. Phys.* **2008**, *106*, 1461–1471.
(48) Huzinaga, S. *J. Chem. Phys.* **1965**, *42*, 1293–1302.
(49) Angeli, C. *Dalton, a molecular electronic structure program, Release 2.0* (2005), see http://www.kjemi.uio.no/software/dalton/dalton.html.
(50) Antusek, A.; Jackowski, K.; Jaszunski, M.; Makulski, W.; Wilczek, M. *Chem. Phys. Lett.* **2005**, *411*, 111–116.
(51) Kamiyama, T.; Seki, N.; Iwasa, H.; Uchida, T.; Ebinuma, T.; Narita, H.; Igawa, N.; Ishii, Y.; Bennington, S.; Kiyanagi, Y. *Phys. B* **2006**, *385−386*, 202–204.
(52) Tse, J. S.; Ratcliffe, C. I.; Powell, B. M.; Sears, V. F.; Handa, Y. P. *J. Phys. Chem. A* **1997**, *101*, 4491–4495.
(53) English, N. J.; Macelroy, J. M. D. *J. Comput. Chem.* **2003**, *24*, 1569–1581.
(54) Wasylishen, R. E.; Bryce, D. L. *J. Chem. Phys.* **2002**, *117*, 10061–10066.
(55) Raynes, W. T. *Specialist Periodical Reports Nuclear Magnetic Resonance*; RSC, 1978; Vol. 7, pp 1−25.
(56) Antusek, A.; Kedziera, D.; Jackowski, K.; Jaszunski, M.; Makulski, W. *Chem. Phys.* **2008**, *352*, 320–326.
(57) Cybulski, H.; Pecul, M.; Sadlej, J. *Chem. Phys.* **2006**, *326*, 431–444.
(58) Hermida-Ramon, J.; Grana, A.; Estevez, C. *Struct. Chem.* **2007**, *18*, 649–652.
(59) Oprea, C. I.; Rinkevicius, Z.; Vahtras, O.; Agren, H.; Ruud, K. *J. Chem. Phys.* **2005**, *123*, 014101.
(60) Sergeyev, N. M.; Sergeyeva, N. D.; Strelenko, Y. A.; Raynes, W. T. *Chem. Phys. Lett.* **1997**, *277*, 142–146.